HHS Public Access

Author manuscript

Nat Commun. Author manuscript; available in PMC 2015 October 28.

Published in final edited form as:

Nat Commun. ; 6: 6934. doi:10.1038/ncomms7934.

Lineage Specification of Ovarian Theca Cells Requires Multi-Cellular Interactions via Oocyte and Granulosa Cells

Chang Liu[1,2], **Jia Peng**[3,4], **Martin M. Matzuk**[3,4], and **Humphrey H-C Yao**[2,*]

[1] Department of Animal Sciences, University of Illinois at Urbana-Champaign, Illinois, USA

[2] Laboratory of Reproductive and Developmental Toxicology, National Institute of Environmental Health Sciences, RTP, North Carolina, USA

[3] Departments of Pathology and Immunology and Molecular and Human Genetics, and Center for Reproductive Medicine, Baylor College of Medicine, Houston, TX 77030

[4] Departments of Molecular and Cellular Biology and Pharmacology, and Center for Drug Discovery, Baylor College of Medicine, Houston, TX 77030

Abstract

Organogenesis of the ovary is a highly orchestrated process involving multiple lineage determinations of ovarian surface epithelium, granulosa cells, and theca cells. While the sources of ovarian surface epithelium and granulosa cells are known, the origin(s) of theca progenitor cells have not been definitively identified. Here we show that theca cells derive from two sources: $Wt1^+$ cells indigenous to the ovary and $Gli1^+$ mesenchymal cells migrated from the mesonephros. These progenitors acquire theca lineage marker *Gli1* in response to paracrine signals Desert hedgehog (*Dhh*) and Indian hedgehog (*Ihh*) from granulosa cells. Ovaries lacking *Dhh*/*Ihh* exhibit theca layer loss, blunted steroid production, arrested folliculogenesis, and failure to form corpora lutea. Production of *Dhh*/*Ihh* in granulosa cells requires Growth differentiation factor 9 (GDF9) from the oocyte. Our studies provide the first genetic evidence for the origins of theca cells and reveal a multicellular interaction critical for the formation of a functional theca.

Ovarian morphogenesis is a highly orchestrated process in which follicles, the basic unit of the ovary, form through an intricate communication between the oocyte, granulosa cells immediately surrounding the oocyte, and theca cells in the mesenchyme. Defects in this process have dire consequences for female reproductive health and fertility [1,2]. The process of folliculogenesis starts with the breakdown of germ cell nests, in which an individual oocyte becomes encased by somatic granulosa cells. As the follicle continues to grow, it

*Correspondence to: humphrey.yao@nih.gov, Phone: 919-541-1095.

Author Contributions

C. L. performed all the experiments; C.L. and H.H.Y designed the study, analyzed data and wrote the paper; P.J. and M.M.M provided *Gdf9* KO ovaries and GDF9 recombinant protein and edited the paper.

Competing Financial Interest Statement

The authors declare no competing financial interests.

Accession Codes

Microarray data have been deposited in GEO under accession code GSE66104.

recruits precursors for the theca cell lineage and completes the process of follicle assembly [2,3]. Theca cells and granulosa cells communicate through epithelial-mesenchymal crosstalk during the course of follicle development [4]. Theca cells produce androgens, which is subsequently converted to estrogens by granulosa cells [2]. Granulosa cell-derived estrogens in turn provide a local feedback loop in regulating androgen production in the theca cells [5]. This unique interaction lays the foundation of the two-cell theory, and illustrates the significance of theca cells in follicular steroid production.Disorders in theca cell differentiation are implicated in ovarian diseases such as polycystic ovary syndrome (PCOS), premature ovarian failure, and ovarian cancers [6-8]. Despite their critical involvement in ovarian development and ovarian pathology, the definitive origin of theca cells has not been identified [9-13].

Theca cells in the mouse ovary do not become morphologically distinguishable until one week after birth in follicles with two layers of granulosa cells (secondary follicles) [2]. However, specification of the theca cell fate already occurs at around time of birth, as neonatal ovaries contain a specified stem/progenitor cell population for theca cells [14].The differentiated theca cells are located in the ovarian mesenchyme, which is separated from granulosa cells and oocytes by a basal membrane [2]. Their histological proximity to granulosa cells led to the hypothesis that recruitment of theca cells from the stroma is regulated by factor(s) produced by granulosa cells [15].A candidate for this factor is Hedgehog (Hh) ligand, a morphogen responsible for lineage specification in many organs [16]. In adult ovaries, Indian hedgehog (*Ihh*) and Desert hedgehog (*Dhh*) are detected in granulosa cells, and their downstream target *Gli1* is expressed in the theca layer [17].In this study, we show that *Gli1* expression starts to appear in the mesenchyme of neonatal ovary after birth, and the neonatal *Gli1*-positive cells represent a progenitor pool for adult theca cells. The *Gli1*-positive theca progenitor population consists of cells from two distinct sources: the fetal ovary and the mesonephros. The fetal ovary- and mesonephros-derived progenitor cells converge in the ovary after birth and commit to the lineage of theca cells by acquiring *Gli1* expression. The expression of *Gli1* in the theca progenitor cells is induced by *Dhh* and *Ihh* in granulosa cells. In the absence of *Dhh* and *Ihh*, theca progenitor cells fail to differentiate into androgen-producing theca cells and ovarian folliculogenesis is disrupted. Furthermore, the Hh ligand production in granulosa cells is regulated by oocyte-specific factor GDF9. Our results demonstrate that the establishment of theca cell lineage requires both granulosa cells and oocyte through multicellular interactions via GDF9 and Hh signaling.

Time course and cell type expression *of Gli1* in the ovary

The expression of *Gli1*, indicated by the presence of beta-galactosidase in the *Gli1-LacZ* reporter mouse, was absent in the ovary before birth and became apparent in the ovary at postnatal day 2 (P2) (Fig. 1a-h). Before birth, *Gli1-LacZ* expression was restricted to the mesenchyme of the mesonephros immediately adjacent to the ovary (Supplementary Fig. 1), particularly in the mesonephric tubules that connect the rete ovarii of the ovary (Fig. 1b). Between birth and P2, the expression of *Gli1* spread from mesonephric tubules into ovarian interstitium (Fig. 1b, c, g and supplementary Fig. 2). By P6, *Gli1-LacZ*-positive cells were found in the mesenchyme surrounding the FOXL2-positive granulosa cells (Fig. 1d, h). This pattern persisted in the adult ovary (Fig. 1i, j).

Mesonephros-derived *Gli1*$^{+}$ cells are a source of theca cells

The close association of *Gli1*-positive cells in the mesonephros and the ovary suggests that *Gli1*-positive cells from the mesonephros could be a source of theca progenitors. To test this hypothesis, we utilized a tamoxifen-induced *Rosa-LSL-tdTomato* lineage-tracing model, in which *Gli1*-positive cells in the mesonephros were labeled exclusively during embryogenesis [18]. We administered a single tamoxifen injection to pregnant mice carrying *Gli1-CreER*^{T2}; *Rosa-LSL-tdTomato* embryos at E12.5, when *Gli1* expression was restricted to the mesonephros [19]. The specificity of this model was confirmed by the lack of fluorescence in control embryos (Supplementary Fig. 3). During fetal life, the tdTomato-positive cells were present specifically in the mesonephros but absent in the ovary (Fig. 2a, b), consistent with endogenous *Gli1* expression pattern (Fig. 1a, e). The tdTomato-positive cells first appeared in the ovary just before birth (Fig. 2c) and a significant number of these cells were observed in the ovary at birth (Fig. 2d and Supplementary Fig. 4). This result demonstrates that the tdTomato-positive cells in the neonatal ovary were derived from the *Gli1*-positive cells in the fetal mesonephros. At two months of age, the mesonephros-derived *Gli1*-positive cells in the ovarian interstitium became steroidogenic theca cells positive for 3βHSD (Fig. 2e-i).

When comparing the *Gli1*-positive cells in the ovary (Fig. 1d, h) with the contribution of *Gli1*-positive cells from the mesonephros (Fig. 2e-i), it became apparent that the mesonephros-derived *Gli1*-positive cells represent a small fraction of the ovarian *Gli1*-positive cell population. The majority of theca cells seem to come from the ovarian mesenchymal cells that become *Gli1*-positive (Fig. 1g, h). This hypothesis was supported by the findings that lineage-labeled ovarian *Gli1*-positive cells at P2 (Fig. 1c, g) became 3βHSD-positive cells in the theca compartment (Fig. 2j-n). Notably, ovarian *Gli1*-positive cells at P2 gave rise to nearly all cells in the theca layer in the adult ovary (Fig. 2j). These results suggest that a small percentage of the theca cells in the adult ovary are derived from the mesonephros whereas the majority of the theca cells must come from progenitor cells that originated in the ovarian mesenchyme.

Ovary-derived *Wt1*$^{+}$ cells are the main source of theca cells

The progenitor cells in the gonadal primordium are thought to be the bona fide source of gonadal somatic cells [20]. When the somatic cell progenitors first appear in the gonad, they express Wilms' tumor 1 (*Wt1*), a transcription factor essential for gonadal formation [21,22].To determine if the gonad-derived *Wt1*-positive cells contribute to the theca cell lineage, we performed similar tamoxifen-induced lineage-tracing experiments by labeling the *Wt1*-postive cells in *Wt1-CreER*^{T2}; *Rosa-LSL-tdTomato* gonads at the onset of sex determination (E10.5). Twenty-four hours after tamoxifen treatment, the lineage-labeled *Wt1*-positive cells were present in the somatic compartment of fetal ovaries overlapped with endogenous WT1 protein (Fig. 3a, d). At one month of age, the ovary-derived *Wt1*-positive cells were located in the ovarian interstitium surrounding the follicles and positive for 3βHSD (Fig. 3c, f). These results indicate that *Wt1* marks a specific pool of steroidogenic precursors in the indifferent gonad before sexual differentiation occurs.To further investigate if these fetal ovary-derived *Wt1*-positive cells become *Gli1*-positive theca progenitor cells after birth (Fig.

1g, 1h), we examined the induction of *Gli1-LacZ* expression in the *Wt1*-positive cells. When the fetal ovary-derived *Wt1*-positive cells began to surround the primary follicles in the medulla of the ovary, they acquired the expression of *Gli1*, indicating that they have committed to the theca cell lineage (Fig. 3b, e).

Transcriptomes of ovary- and mesonephros-derived *Gli1*$^{+}$ cells

Fetal ovary-derived *Wt1*-positive cells and mesonephros-derived *Gli1*-positive cells appear to represent two different populations of theca cells. Fetal ovary-derived *Wt1*-positive cells were found in the entire theca in the adult ovary, whereas mesonephros-derived *Gli1*-positive cells were located preferentially to the basal lamina (Supplementary Fig. 5), a region that contains predominantly steroidogenic cells [3]. This observation leads to the hypothesis that these two cellular sources of progenitors represent unique populations in the theca. We isolated mesonephros-derived *Gli1*-positive cells (Fig. 2e) and neonatal ovary-derived *Gli1*-positive cells (Fig.2j) by FACS from 2 month-old mice, and compared their transcriptomes (Fig. 3g). The microarray analysis indicated that mesonephros-derived theca cells exhibit a transcriptome distinctly different from that of the ovary-derived *Gli1* population. Many of the genes enriched in the mesonephros-derived theca cells were associated with steroidogenesis, including *Star*, *Cyp11a1*, *Cyp17a1*, and *Lhcgr* (Fig. 3h). The steroidogenic activity of these cells was also confirmed by immunostaining with 3βHSD (Supplementary Fig. 6). In contrast, the ovary-derived *Gli1*-positive cells exhibited higher expression of *Esr1* (Estrogen receptor 1), *Wt1*, and genes implicated in cell growth and proliferation (Supplementary Table 1), consistent with their ubiquitous distribution within the theca layer.These results demonstrate that ovary-derived *Gli1*-positive cells represent a broad mesenchymal cell population(s), whereas the mesonephros-derived *Gli1*-positive cells contribute to the steroidogenic cell population in the theca.

Granulosa cells are sources of Hedgehog ligands *Dhh* and *Ihh*

The identification of *Gli1* as a theca cell lineage marker raises the question: what signal(s) specify theca cell lineage and induces *Gli1* expression? *Gli1* is a known downstream target of the Hh pathway [19]. We first examined whether activation of the Hh pathway is responsible for inducing *Gli1* expression by culturing fetal ovaries in the presence or absence of the Hh inhibitor cyclopamine [23]. Cyclopamine treatment inhibited *Gli1* expression in the ovaries compared to the controls (Fig. 4a-c), indicating that *Gli1* expression is induced by the canonical Hh pathway. In search of the Hh ligands that may be responsible for activating the Hh pathway, we examined mRNA expression of Desert Hedgehog (*Dhh*), Indian Hedgehog (*Ihh*), and Sonic hedgehog (*Shh*) in the ovary before (E17.5) and after (PND3) the appearance of *Gli1*. Expression of *Dhh* and *Ihh* was low in the ovary before birth and significantly increased at PND3, corresponding to the onset of *Gli1* expression (Fig. 4d). Expression of *Shh* was undetectable in ovaries at both stages (Supplementary Fig. 7). To identify which somatic cell type(s) produce *Dhh* and *Ihh*, we isolated theca progenitor cells (*Gli1-CreER*^{T2}; *Rosa-LSL-tdTomato*) and granulosa cells (*Foxl2-CreER*^{T2}; *Rosa-LSL-tdTomato*) from perinatal ovaries by FACS (Supplementary Fig. 8). We found that the Hh downstream targets *Gli1* and *Ptch1* were highly enriched in theca progenitor cells, whereas Hh ligands *Dhh* and *Ihh* were found predominantly in granulosa

cells (Fig. 4e).These results implicate a novel regulation of theca cell differentiation by granulosa cells through the Hedgehog signaling pathway.

Loss of *Dhh* and *Ihh* abolishes theca cell differentiation

Female *Dhh*-deficient mice are fertile and exhibit normal ovarian development [24], suggesting that the other Hh ligands, such as *Ihh*, may compensate for the loss of *Dhh* during folliculogenesis. Most of the *Ihh* global deficient embryos die before birth [25], therefore precluding the analysis of the ovary in the adult. To investigate whether *Dhh* and *Ihh* together regulate theca cell development, we generated *Dhh*/*Ihh* double knockout mice (Hereafter referred as *Dhh*/*Ihh* DKO), in which both *Dhh* and *Ihh* were ablated from *Sf1*-positive gonadal somatic cells (*Sf1-Cre; Ihh* $^{f/-}$*; Dhh* $^{-/-}$) [26]. Although *Sf1-cre* is known to be active in the pituitary, we do not expect that it affects pituitary functions based on the fact that *Dhh* and *Ihh* are not expressed in the pituitary [16,27]. Ovaries deficient in either *Dhh* or *Ihh* alone exhibited normal folliculogenesis (Supplementary Fig. 9). However, *Dhh*/*Ihh* DKO ovaries were significantly smaller in size and irregular in shape compared to the control (Fig.5a, b). In contrast to the normal progression of folliculogenesis and the presence of corpora lutea in adult control ovaries, *Dhh*/*Ihh* DKO ovaries lacked corpora lutea, and follicles failed to progress beyond preantral follicle stage, suggesting that ovulation did not occur (Fig. 5c-f). Antral follicles were rarely found in the DKO ovaries and if they were present, they appeared cystic and hemorrhagic (Fig. 5g, h). In addition to a loss of theca, as determined by α-SMA, a marker for smooth muscle cells in the theca layer (Fig. 6a, b) [28], CYP17A1-positive androgen-producing theca cells were also absent in the mesenchyme of DKO ovaries (Fig. 6c, d). Furthermore, steroidogenic genes, including *Nr5a1*, *Star*, *Cyp11a1*, and *Hsd3b1* (Fig. 6e), were significantly downregulated along with a decrease in serum levels of dehydroepiandrosterone (DHEA), testosterone, and progesterone in the DKO mice (Fig. 6f). These results altogether support the model that *Dhh* and *Ihh* from granulosa cells are responsible for the establishment of theca cell linage. In the absence of *Dhh* and *Ihh*, theca cell layer failed to form and preantral follicles were unable to develop further.

Oocyte-derived GDF9 regulates *Dhh /Ihh* in granulosa cells

Next we investigated what signal induces the production of Hh ligands in the granulosa cells. Functions of granulosa cells are regulated not only systemically by hormone signals from the pituitary, but also locally via factors produced in the oocytes [1]. Without the oocyte, follicle formation never occurs [29]. To test if oocytes play a role in Hh ligand production, we treated pregnant females with busulfan, a chemotherapeutic drug known to induce oocyte death in the embryos [30,31]. The specificity of *in utero* busulfan treatment on oocytes was confirmed by a complete abolishment of oocytes, coincident with normal establishment of FOXL2-positive granulosa cell population in ovaries of busulfan-treated pups (Supplementary Fig. 10). In the oocyte-depleted ovaries, expression of *Dhh*, *Ihh*, and *Gli1* were significantly downregulated (Fig. 7a and Supplementary Fig. 10), suggesting that oocyte-derived factor(s) contributes to *Dhh* and *Ihh* production in granulosa cells. One potential candidate of such factor is Growth differentiation factor 9 (Gdf9), an oocyte-specific factor essential for folliculogenesis [1,32]. In neonatal *Gdf9* knockout ovaries,

expression of *Dhh* and *Ihh* was significantly reduced, and *Gli1* expression was also decreased (Fig. 7b). When recombinant GDF9 was supplemented to oocyte-depleted ovaries (Busulfan-treated) in culture, it increased mRNA expression of *Ihh*, *Dhh*, and subsequent *Gli1* (Fig. 7c), further supporting the role of oocyte-derived GDF9 in stimulating *Dhh* and *Ihh* production in granulosa cells and subsequent appearance of *Gli1*-positive theca progenitor cells (Fig, 7d). To exclude the possibility that GDF9 might directly act on theca cells, we examined the expression of *Gdf9* in the DKO ovaries and it was not different from those of control animals (Supplementary Fig. 11).

Discussion

We provide the first genetic evidence for the origins of theca progenitor cells: *Wt1*-positive cells intrinsic to ovary and *Gli1*-positive cells in the mesonephros, It is not clear why two sources of theca cell progenitors are required for follicle development and we speculate that this phenomenon may relate to temporal and spatial characteristics of follicle development. Two classes of primordial follicles are present in the ovary: the primordial follicles (first wave) that are activated immediately after birth in the medulla of the ovary, and the primordial follicles (second wave) that are gradually activated later in adulthood in ovarian cortex [33].Granulosa cell precursors that comprise each primordial follicle appear to be heterogeneous populations. The pre-granulosa cells that are specified during fetal stage contribute to the first wave of primordial follicles in the medulla of the ovary immediately after birth. On the other hand, the granulosa cells in the cortex of postnatal ovaries participate in the second wave of primordial follicles later in adulthood [34].Along this line of evidence, our finding demonstrated that theca cells also arise from two distinct sources. It is possible that the two sources of theca progenitor cells are involved in the two waves of follicular development. The mesonephros-derived *Gli1*-positive cells are first seen in the medulla of the neonatal ovary where the first wave of follicular development occurs. This observation suggests that the mesonephros-derived theca progenitor cells could be implicated in the initiation of the first wave of folliculogenesis. It is not clear whether the GDF9/Hedgehog signaling is controlling both classes of follicles, or a certain population. However, if GDF9/Hedgehog signaling controls only one class of follicles but not the other, one would assume that the other class of follicles should develop normally with the formation of a functional theca in the absence of GDF9 or Hedgehog signaling. In fact, in the *Dhh/Ihh* DKO ovaries, the theca layer failed to differentiate in all follicles, indicating that both classes of follicles are affected by the loss of *Dhh* and *Ihh*.

Although *Dhh* and *Ihh* appear to be downstream targets of GDF9, the ovarian phenotypes of *Gdf9* KO ovaries differ from those observed in *Dhh/Ihh* dKO ovaries. The follicles in the *Gdf9* KO ovaries arrest at primary stage, whereas follicles in *Dhh/Ihh* dKO ovaries develop beyond the primary stage and arrest at the preantral stage. The difference in phenotypes reveals two important findings: First, DHH/IHH signaling pathway plays a specific role in theca cell differentiation and second, GDF9, the factor responsible for the production of *Dhh* and *Ihh*, has a broader function in follicle development. The identities of other players that act downstream of GDF9 remains to be identified.

In contrast to the long-standing assumption that theca cells derive exclusively from within the ovarian stroma [13], we reveal an extra-ovarian source of *Gli1*-positive cells from the mesonephros that contributes to the adult theca cell lineage. In addition, we demonstrate that *Wt1* marks a specific pool of steroidogenic precursors in the bipotential gonad before sexual differentiation occurs. These theca progenitor cells commit to theca cell lineage via signals from oocyte (GDF9) and granulosa cells (DHH and IHH). Oocyte-specific factor GDF9 stimulates Hh ligand production in granulosa cells, which in turn induces the differentiation of *Gli1*-positive theca progenitor cells (Fig. 7d). Given that disorders in theca cell differentiation are implicated in ovarian diseases such as polycystic ovary syndrome, premature ovarian failure and ovarian cancers [6-8,35,36], our discovery of the origins of theca cells and the mechanism underlying their appearance not only fill a critical void in basic ovarian biology, but also serve as novel entry points to understand how theca cell-related pathology affects female reproductive health.

Methods

Animals breeding

Gli1-LacZ (#008211), *Gli1-CreER^{T2}* (#007913), *Wt1-CreER^{T2}* (#010912), *Foxl2-CreER^{T2}* (#015854), Rosa-LSL-tdTomato (#007905), *Dhh$^{+/-}$* (#002784), *Ihh$^{+/-}$* (#004290) mice were purchased from the Jackson Laboratory (Bar Harbor, ME). *Sf1-Cre* and *Ihh $^{floxed/floxed}$* mice were kind gifts from Dr. Keith Parker (UT Southwestern Medical Center) and Dr. Francesco DeMayo (Baylor College of Medicine), respectively. Female mice were housed with male mice overnight and checked for the presence of vaginal plug the next morning. The day when the vaginal plug was detected was considered embryonic day (E) 0.5. The day of birth was considered postnatal day 1 (P1).All animal procedures were approved by the National Institute of Environmental Health Sciences (NIEHS) Animal Care and Use Committee and are in compliance with a NIEHS-approved animal study proposal. All experiments were performed on at least three animals for each genotype.

Busulfan treatment

Pregnant CD-1 females were injected intraperitoneally (IP) at E10.5 with 40 mg/kg of busulfan (Sigma) dissolved in 50% DMSO, or an equivalent volume of 50% DMSO as the vehicle control.

Tamoxifen treatment

CreER^{T2} activity was induced by IP injection of 1 mg tamoxifen (T-5648, Sigma-Aldrich, St. Louis, MO) per mouse in corn oil, receptively. For the vehicle control, an equivalent volume of corn oil was injected. No overt teratological effects were observed after tamoxifen administration under these conditions.

Immunohistochemistry and histological analysis

For immunohistochemistry on frozen sections, ovaries were fixed in 4% paraformaldehyde in PBS at 4°C overnight, dehydrated through a sucrose gradient, embedded, and cryosectioned at 10 μm increments. After preincubating with 5% normal donkey serum in PBS for 1 hour, the sections were then incubated with either anti-FOXL2 (1:500, a gift from

Dr. Dagmar Wilhelm, Monash University, Australia), anti-PECAM-1 (1:500, BD Biosciences, USA), anti-3βHSD (1:500, CosmoBio Co.Ltd, Japan), anti-β-galactosidase (1:1000, Abcam, USA), anti-TRA98 (1:1000, MBL international, USA), or anti-WT1 (1:300, Abcam, USA) primary antibodies in PBS-Triton X-100 solution with 5% normal donkey serum at 4°C overnight. The sections were then washed and incubated in the appropriate secondary antibody (1:500; Invitrogen, USA) before mounting in Vector Mount with DAPI (Vector Labs). For paraffin-embedded tissues, the sections were dewaxed and rehydrated in a series of alcohol to PBS. The slides were pretreated in 0.1 mM citric acid for 20 min in the microwave, incubated with anti-αSMA (1:500, Abcam, USA) and anti-CYP17A1 (1:100, Santa Cruz, USA). Slides were imaged under a Leica DMI4000 confocal microscope.For histological analysis, the samples were fixed in 4% paraformaldehyde in PBS at 4°C overnight, dehydrated through an ethanol gradient, and embedded in paraffin wax. Sections were stained with hematoxylin/eosin or PAS/ hematoxylin, and were scanned using Aperio ScanScope XT Scanner (Aperio Technologies, Inc., CA, USA) for digital image analysis.

LacZ staining

The LacZ staining solution was made by dissolving X-gal (Invitrogen, CA) into Dimethylformamide to make 40mg/ml stock solution. The working solution was further prepared by diluting the stock solution to 1mg/ml in pre-warmed tissue stain base solution (Chemicon, MA) [37]. Fresh tissues were stained in the LacZ staining solution at 37°C for 2-3 hours followed by fixation in 4% paraformaldehyde/PBS at 4°C overnight. For further histological analysis, samples after LacZ staining were embedded in paraffin following the sectioning procedure listed above. The sections were counterstained with Fast Red (Sigma).

Gene expression analysis

Total RNA was isolated from ovaries using the PicoPure RNA isolation kit (Arcturus, Mountain View, CA) according to the manufacturer's protocol. The cDNA preparation was synthesized using random hexamers and the Superscript II cDNA synthesis system (Invitrogen Corp., Carlsbad, CA) following the manufacturer's instruction. Gene expression was analyzed by real-time PCR using Bio-Rad CFX96™ Real-Time PCR Detection system. Taqman gene-expression probes (*Gli1*: Mm00494654_m1, *Ptch1*: Mm00436026_m1, *Ihh*: Mm00439613_m1, *Shh*: Mm00436528_m1, *Dhh*: Mm01310203_m1, *Foxl2*: Mm00843544_m1, *Star*: Mm00441558_m1, *Cyp11a1*: Mm00490735_m1, *Cyp17a1*: Mm00484040_m1, *Lhcgr*: Mm00442931_m1, *Hsd3b1*: Mm01261921_mH, *Gdf9*: Mm00433565_m1, *Nr5a1*: Hs01018738_m1, *Cyp19a1*: Mm00484049_m1) were used to detect the fold changes of the transcripts. Fold changes in gene expression were determined by quantitation of cDNA from target (treated) samples relative to a calibrator sample (control). All real-time PCR analyses were performed in duplicate, and the results were reported from at least three independent experiments. The relative fold change of transcript was calculated using the mathematical model of Pfaffl [38] and was normalized to *18S* rRNA (Mm03928990_g1), *Gapdh* (Mm99999915_g1) or *Gata4* (Mm00484689_m1) as an endogenous reference.

Microarray analysis

Gene expression analysis was conducted using Affymetrix Mouse Genome 430 2.0 GeneChip® arrays (Affymetrix, Santa Clara, CA). Four microliters of total RNA (due to varying concentrations among samples) was amplified as directed in the WT-Ovation Pico RNA Amplification System protocol, and labeling with biotin following the Encore Biotin Module. 4.6 μg of amplified biotin-aRNAs were fragmented and hybridized to each array for 18 hours at 45°C in a rotating hybridization. Array slides were stained with streptavidin/phycoerythrin utilizing a double-antibody staining procedure and then washed for antibody amplification according to the GeneChip Hybridization, Wash and Stain Kit and user manual following protocol FS450-0004. Arrays were scanned in an Affymetrix Scanner 3000 and data was obtained using the GeneChip® Command Console Software (AGCC; Version 1.1). The microarray raw data were analyzed using the Partek Genomic Suite Software (St. Louis, Missouri). Two-way Anova was performed to determine the statistical significance between the means. The gene list was filtered with fold-change cutoff of 1.4 and an unadjusted $p<0.05$. Microarray data have been deposited in GEO under accession code GSE66104.

Organ culture

Ovaries from E18.5 embryos (Fig. 4a-c, Fig. 7a&c and Supplementary Fig. 10) were cultured for 3 days on Millicell-PC membrane inserts (0.4 μm pore size; 30 mm diameter; Millipore corp., Medford, MA) with medium filling only the lower chamber [39]. 8-10 ovaries were placed on each membrane, with one drop of medium on each ovary. For culture with the Hh inhibitor, cyclopamine [23] (25 μM, Sigma) was added to the ovary culture at the beginning of the culture for 3 days. For culture with GDF9 recombinant protein [40], the protein (60 ng/ml) was added to the ovary culture at the last day of culture 24 hours prior to the collection.The medium for organ culture was DMEM/F12 (1:1) + L-Glutamine + 15mM HEPES (Invitrogen) supplemented with 50 μg/ml penicillin G/streptomycin sulfate, and 5% (vol/vol) fetal bovine serum (FBS). The culture medium was refreshed every other day, and after 3 days of culture, the ovaries were harvested for RNA isolation for qPCR analysis, or were fixed in 4% paraformaldehyde/PBS for histological analysis as described above.

Steroid Hormone Multiplex Immunoassay

Mice were not staged for estrus cycle at the time of sample collection. Serum samples were collected at various times, aliquoted and stored at −80°C until analyzed. Serum samples were assayed for DHEA, Estradiol, Progesterone, and Testosterone using the Steroid Hormone Panel kit (cat # N45CB-1) from MSD (Meso Scale Discovery, Gaithersburg, Maryland, USA) according to manufacturer's protocols. The Steroid Hormone Panel utilizes a competitive immunoassay format. Briefly, a 96 well custom designed plate that had been precoated with capture antibodies on spatially distinct spots was blocked with blocking solution for 1 hr. at room temperature with constant shaking at 700 rpm. After washing 3x with PBS-T buffer, samples and standards were added to appropriate wells of the MSD plate and incubated for 2 hrs at RT with constant shaking. After incubation of the samples, a mixture of MSD SULFOTAG™ labeled tracers are added to each well. The tracers compete with analytes in the samples for binding on the immobilized antibodies generating a signal

for each assay this is inversely proportional to the analyte concentration. After incubating with the tracers, the plate was washed again 3x with PBS-T, pat dried, and 150 µl of 1x Read Buffer was added to each well. The plate was immediately analyzed on the Sector Imager 2400 System (MSD). The instrument measures intensity of emitted light to afford a quantitative measure of DHEA, Estradiol, Progesterone, and Testosterone in the sample. Testosterone standard is not supplied with the MSD kit, it was purchased separately from Steraloids (cat # A6950) (Newport, RI, USA) and used in the range from 16 ng/mL to 0.1 ng/mL. All the samples were run on the same plate. The intra-array %CV (n=7) is 3.99 for DHEA, 7.63 for testosterone and 13.32 for progesterone.

Statistical analysis

Data were analyzed using Prism (Version 6, GraphPad Software) by two-tailed Student's *t*-test. Values are presented as mean±s.e.m. A minimal of 3 biological replicates was used for each experiment.

Supplementary Material

Refer to Web version on PubMed Central for supplementary material.

Acknowledgments

We thank Dr. Keith Parker (UT Southwestern Medical Center) for the *Sf1-Cre* mice, Dr. Francesco DeMayo (Baylor College of Medicine) for the *Ihh* $^{floxed/floxed}$ mouse strain, and Dr. Dagmar Wilhelm (Monash University) for the anti-FOXL2 antibody. We thank the Comparative Medicine Branch, the Flow Cytometry Center, the Cellular & Molecular Pathology Branch (the Digital Imaging/Analysis Lab, the Clinical Pathology Lab and the Pathology Support Group), and the Molecular Genomics Core at NIEHS for the technical support. We also thank Dr. Mitch Eddy, Dr. Kenneth Korach and other lab members for their critical comments on the manuscript. This research was supported by the Intramural Research Program (ES102965) to H.H-C.Y of the NIH, National Institute of Environmental Health Sciences and NIH Graduate Partnerships Program and the Eunice Kennedy Shriver National Institute of Child Health and Human Development (R01 HD033438 to M.M.M.).

References

1. Matzuk MM, Lamb DJ. The biology of infertility: research advances and clinical challenges. Nat Med. 2008; 14:1197–1213. doi:10.1038/nm.f.1895. [PubMed: 18989307]
2. Edson MA, Nagaraja AK, Matzuk MM. The mammalian ovary from genesis to revelation. Endocr Rev. 2009; 30:624–712. doi:10.1210/er.2009-0012. [PubMed: 19776209]
3. Hirshfield AN. Development of follicles in the mammalian ovary. Int Rev Cytol. 1991; 124:43–101. [PubMed: 2001918]
4. Nilsson E, Skinner MK. Cellular Interactions That Control Primordial Follicle Development and Folliculogenesis. Journal of the Society for Gynecologic Investigation. 2001; 8:S17–S20. doi: 10.1177/10715576010080010 6. [PubMed: 11223364]
5. Roberts AJ, Skinner MK. Mesenchymal-epithelial cell interactions in the ovary: estrogen-induced theca cell steroidogenesis. Mol Cell Endocrinol. 1990; 72:R1–5. [PubMed: 2272402]
6. Magoffin DA. The ovarian androgen-producing cells: a 2001 perspective. Rev Endocr Metab Disord. 2002; 3:47–53. [PubMed: 11883104]
7. Shiina. Premature ovarian failure in androgen receptor-deficient mice. et al. Proc Natl Acad Sci U S A. 2006; 103:224–229. doi:0506736102 [pii]10.1073/pnas.0506736102.
8. Wang PH, Chang C. Androgens and ovarian cancers. Eur J Gynaecol Oncol. 2004; 25:157–163. [PubMed: 15032272]
9. Erickson GF, Magoffin DA, Dyer CA, Hofeditz C. The ovarian androgen producing cells: a review of structure/function relationships. Endocr Rev. 1985; 6:371–399. [PubMed: 3896767]

10. Quattropani SL. Morphogenesis of the ovarian interstitial tissue in the neonatal mouse. The Anatomical record. 1973; 177:569–583. doi:10.1002/ar.1091770410. [PubMed: 4762731]
11. Peters H, Pedersen T. Origin of follicle cells in the infant mouse ovary. Fertil Steril. 1967; 18:309–313. [PubMed: 6024076]
12. Hirshfield A. Theca cells may be present at the outset of follicular growth. Biology of reproduction. 1991; 44:1157–1162. [PubMed: 1873389]
13. Young JM, McNeilly AS. Theca: the forgotten cell of the ovarian follicle. Reproduction. 2010; 140:489–504. doi:REP-10-0094 [pii]10.1530/REP-10-0094. [PubMed: 20628033]
14. Honda A, et al. Isolation, characterization, and in vitro and in vivo differentiation of putative thecal stem cells. P Natl Acad Sci USA. 2007; 104:12389–12394. doi:10.1073/pnas.0703787104 .
15. Liu CF, Liu C, Yao HH. Building pathways for ovary organogenesis in the mouse embryo. Curr Top Dev Biol. 2010; 90:263–290. doi:S0070-2153(10)90007-0 [pii]10.1016/S0070-2153(10)90007-0. [PubMed: 20691852]
16. Varjosalo M, Taipale J. Hedgehog: functions and mechanisms. Genes Dev. 2008; 22:2454–2472. doi:22/18/2454 [pii]10.1101/gad.1693608. [PubMed: 18794343]
17. Wijgerde M, Ooms M, Hoogerbrugge JW, Grootegoed JA. Hedgehog signaling in mouse ovary: Indian hedgehog and desert hedgehog from granulosa cells induce target gene expression in developing theca cells. Endocrinology. 2005; 146:3558–3566. doi:en.2005-0311 [pii]10.1210/en.2005-0311. [PubMed: 15878962]
18. Liu C, Paczkowski M, Othman M, Yao HHC. Investigating the Origins of Somatic Cell Populations in the Perinatal Mouse Ovaries Using Genetic Lineage Tracing and Immunohistochemistry. Germline Development: Methods and Protocols. 2012; 825:211–221. doi:Doi 10.1007/978-1-61779-436-0_16.
19. Barsoum I, Yao HH. Redundant and differential roles of transcription factors Gli1 and Gli2 in the development of mouse fetal Leydig cells. Biol Reprod. 2011; 84:894–899. doi:10.1095/biolreprod.110.088997. [PubMed: 21209421]
20. Gillman, J. The development of the gonads in man, with a consideration of the role of fetal endocrines and the histogenesis of ovarian tumors. 1948.
21. Armstrong JF, Pritchard-Jones K, Bickmore WA, Hastie ND, Bard JB. The expression of the Wilms' tumour gene, WT1, in the developing mammalian embryo. Mech Dev. 1993; 40:85–97. [PubMed: 8382938]
22. Kreidberg JA, et al. WT-1 is required for early kidney development. Cell. 1993; 74:679–691. doi:0092-8674(93)90515-R [pii]. [PubMed: 8395349]
23. Taipale J, et al. Effects of oncogenic mutations in Smoothened and Patched can be reversed by cyclopamine. Nature. 2000; 406:1005–1009. doi:10.1038/35023008. [PubMed: 10984056]
24. Bitgood MJ, Shen L, McMahon AP. Sertoli cell signaling by Desert hedgehog regulates the male germline. Curr Biol. 1996; 6:298–304. [PubMed: 8805249]
25. St-Jacques B, Hammerschmidt M, McMahon AP. Indian hedgehog signaling regulates proliferation and differentiation of chondrocytes and is essential for bone formation. Genes Dev. 1999; 13:2072–2086. [PubMed: 10465785]
26. Bingham NC, Verma-Kurvari S, Parada LF, Parker KL. Development of a steroidogenic factor 1/Cre transgenic mouse line. Genesis. 2006; 44:419–424. doi:10.1002/dvg.20231. [PubMed: 16937416]
27. Ingham PW, McMahon AP. Hedgehog signaling in animal development: paradigms and principles. Genes Dev. 2001; 15:3059–3087. doi:10.1101/gad.938601. [PubMed: 11731473]
28. Ren Y, Cowan RG, Harman RM, Quirk SM. Dominant activation of the hedgehog signaling pathway in the ovary alters theca development and prevents ovulation. Mol Endocrinol. 2009; 23:711–723. doi:me.2008-0391 [pii]10.1210/me.2008-0391. [PubMed: 19196835]
29. McLaren A. Development of the mammalian gonad: the fate of the supporting cell lineage. Bioessays. 1991; 13:151–156. doi:10.1002/bies.950130402 . [PubMed: 1859392]
30. Bucci LR, Meistrich ML. Effects of busulfan on murine spermatogenesis: cytotoxicity, sterility, sperm abnormalities, and dominant lethal mutations. Mutat Res. 1987; 176:259–268. [PubMed: 3807936]

31. Hemsworth BN, Jackson1 H. Effect of 'busulphan' on the foetal gonad. Nature. 1962; 195:816–817. [PubMed: 13906380]
32. Dong J, et al. Growth differentiation factor-9 is required during early ovarian folliculogenesis. Nature. 1996; 383:531–535. doi:10.1038/383531a0. [PubMed: 8849725]
33. Zheng W, et al. Two classes of ovarian primordial follicles exhibit distinct developmental dynamics and physiological functions. Human molecular genetics. 2013 doi:10.1093/hmg/ddt486.
34. Mork L, et al. Temporal differences in granulosa cell specification in the ovary reflect distinct follicle fates in mice. Biol Reprod. 2012; 86:37. doi:10.1095/biolreprod.111.095208. [PubMed: 21976597]
35. McAllister JM, et al. Overexpression of a DENND1A isoform produces a polycystic ovary syndrome theca phenotype. Proc Natl Acad Sci U S A. 2014; 111:E1519–1527. doi:10.1073/pnas.1400574111. [PubMed: 24706793]
36. Husebye ES, Lovas K. Immunology of Addison's disease and premature ovarian failure. Endocrinol Metab Clin North Am. 2009; 38:389–405. ix, doi:10.1016/j.ecl.2009.01.010. [PubMed: 19328418]
37. Franco HL, et al. Constitutive activation of smoothened leads to female infertility and altered uterine differentiation in the mouse. Biology of reproduction. 2010; 82:991–999. doi:10.1095/biolreprod.109.081513. [PubMed: 20130264]
38. Pfaffl MW. A new mathematical model for relative quantification in real-time RT-PCR. Nucleic Acids Res. 2001; 29:e45. [PubMed: 11328886]
39. O'Brien MJ, Pendola JK, Eppig JJ. A revised protocol for in vitro development of mouse oocytes from primordial follicles dramatically improves their developmental competence. Biology of reproduction. 2003; 68:1682–1686. doi:10.1095/biolreprod.102.013029. [PubMed: 12606400]
40. Peng J, et al. Growth differentiation factor 9:bone morphogenetic protein 15 heterodimers are potent regulators of ovarian functions. Proc Natl Acad Sci U S A. 2013; 110:E776–785. doi:10.1073/pnas.1218020110. [PubMed: 23382188]

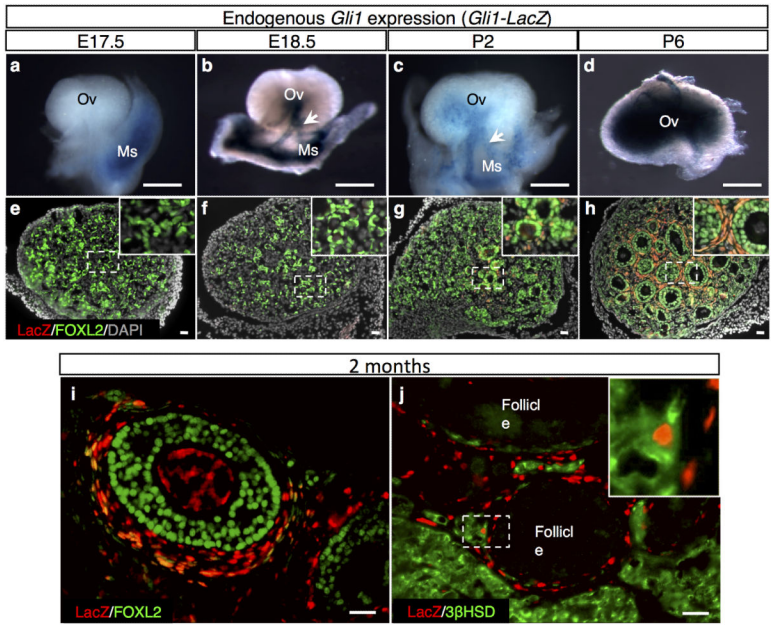

Figure 1. Time course analyses of *Gli1* expression in the ovary

a-j, Expression of *Gli1-LacZ* in the ovaries was detected by whole mount beta-galactosidase staining (a-d) or fluorescent immunohistochemistry for *Gli1*-positive cell marker LacZ, granulosa cell marker FOXL2, steroidogenic cell marker 3bHSD and nuclear counterstain DAPI at E17.5 (a, e), E18.5 (b, f), P2 (c, g), P6 (d, h) and 2 months (i, j). The insets are higher magnification of the outlined areas in e-h and j. Arrow, mesonephric tubules; E, embryonic day; Ov, ovary; Ms, mesonephros; P, postnatal day. n=3-5 for each *Gli1-LacZ* specimen. Scale bar: a-d, 500 mm; e-j, 25 mm.

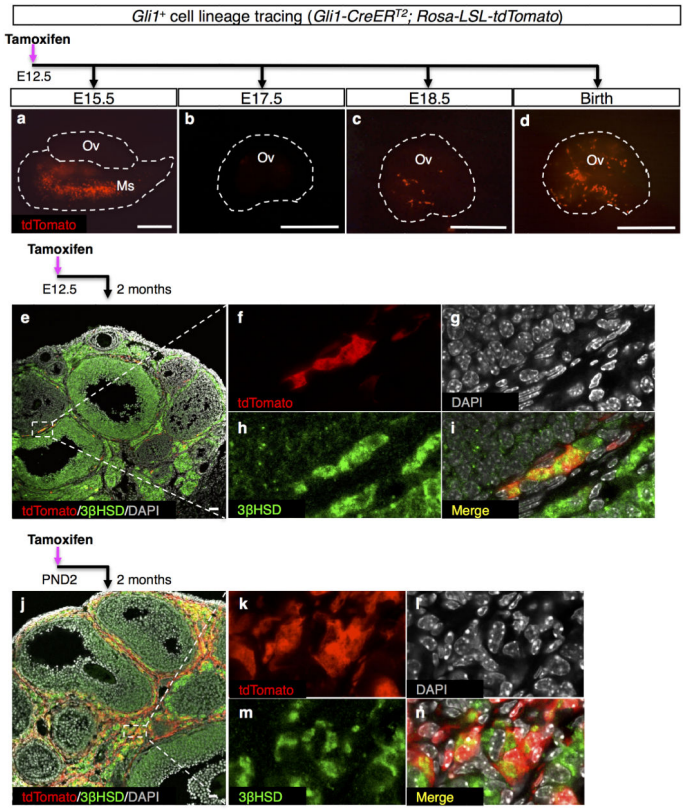

Figure 2. Lineage-tracing experiments for the *Gli1*-positive cells in the ovary and mesonephros

a-n, Lineage-tracing of the *Gli1*-positive cells in the *Gli1-CreER^{T2}; Rosa-LSL-tdTomato* embryos was induced by tamoxifen (TM) administration at E12.5 (mesonephros-derived, a-i), or at P2 (neonatal ovary-derived, j-n). The ovaries were examined at different stages of development for tdTomato, steroidogenic marker 3bHSD, and DAPI. The staining for 3βHSD was observed not only in theca cell layer but also in granulosa cells in large antral follicles. f-i and k-n are higher magnification images of the outlined areas in e and j in single fluorescence channels. n=3-6 for each *Gli1-CreER^{T2}; Rosa-LSL-tdTomato* specimen. Scale bar: a-d, 500 mm; e&i, 25 mm.

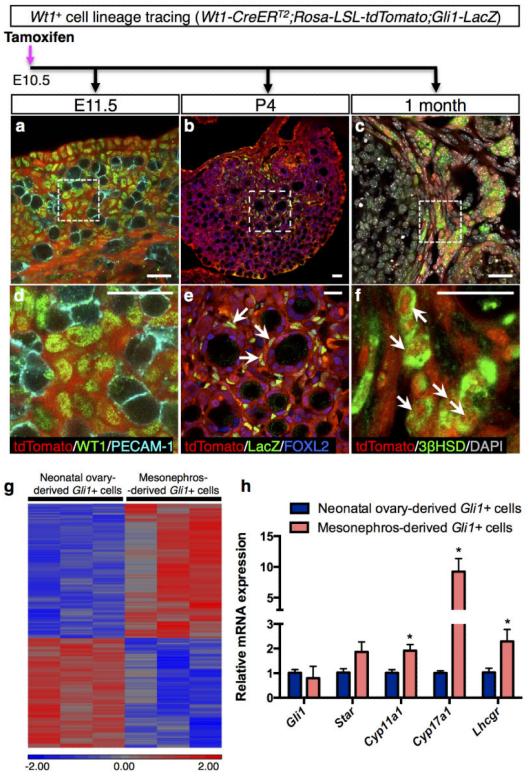

Figure 3. Lineage-tracing experiments for the *Wt1*-positive cells in the ovary and transcriptome analysis of the mesonephros- and ovary-derived *Gli1*-positive cells

a-c, Lineage-tracing of the fetal ovary-derived *Wt1*-positive cells in the *Wt1-CreER^{T2}; Rosa-LSL-tdTomato; Gli1-LacZ* embryos was induced by tamoxifen (TM) administration at E10.5. The ovaries were analyzed at different stages of development (E11.5, P4, and 1 month) by fluorescent immunohistochemistry for tdTomato, WT1, germ cell marker PECAM-1, LacZ, granulosa cell marker FOXL2, steroidogenic marker 3bHSD, and DAPI. E= embryonic day; P= postnatal day. **d-f**, are higher magnification of the outlined areas in (a-c). Arrows indicate fetal ovary-derived *Wt1*-positive cells.n=3-4 for each specimen. Scale bar: 25 mm. **g**, Microarray analyses of 3 independent pools of the mesonephros-derived and the neonatal ovary-derived *Gli1*-positive cells. All cells were isolated from the adult ovaries of *Gli1-CreER^{T2}; Rosa-LSL-tdTomato* mice at 2 months of age. **h**, qPCR analysis of *Gli1* and markers of theca cell steroidogenesis (*Star*, Cyp11a1, Cyp17a1, and *Lhcgr*) in the mesonephros-derived (n=3) and the neonatal ovary-derived *Gli1*-positive cells (n=3). *P < 0.05; Two-tailed Student's *t*-test. Values are presented as means±s.e.m.

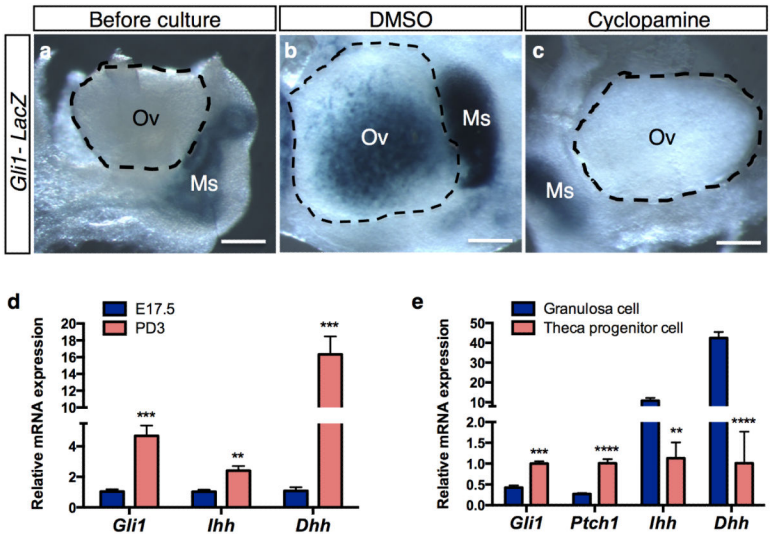

Figure 4. *Dhh* and *Ihh* in the granulosa cells are responsible for *Gli1* expression in the theca progenitor cells

a-c, Effects of the Hedgehog inhibitor cyclopamine on expression of *Gli1-LacZ* in the ovary. *Gli1-LacZ* ovaries (E18.5) were cultured in the presence or absence of cyclopamine (25 μM) for 3 days followed by LacZ staining (blue). Ov= ovary; Ms= mesonephros. n=5-6 for each specimen. Scale bar: 500 mm. **d**, qPCR analysis of *Gli1*, *Ihh* and *Dhh* mRNA expression in E17.5 (n=5) and PD3 (n=5) ovaries. **e**, qPCR analysis of *Gli1*, *Ptch1*, *Ihh*, and *Dhh* mRNA expression in granulosa cells (n=5) and theca progenitor cells (n=3). Cells isolated from a pair of ovaries were pooled as n of 1. (see Supplementary Fig. 8 for details). **P < 0.01; ***P < 0.001; ****P< 0.0001; Two-tailed Student's *t*-test. Values in all graphs are presented as means±s.e.m.

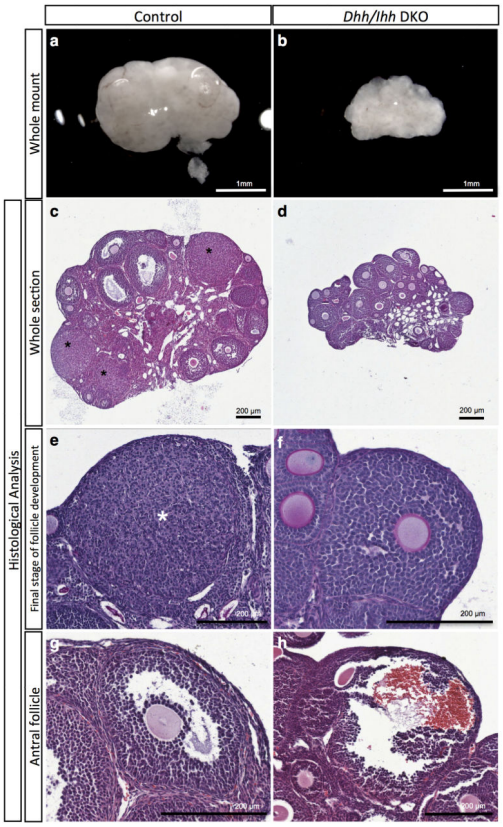

Figure 5. Loss of *Dhh* and *Ihh* results in defective folliculogenesis in the ovary

a-h, Whole mount light-field microscopic images (a-b) **and** histological analysis of the ovaries (c-h) from control (*Sf1-Cre; Ihh* $^{f/+}$*; Dhh*$^{+/-}$) and *Dhh/Ihh* DKO mice (*Sf1-Cre; Ihh* $^{f/-}$*; Dhh* $^{-/-}$) at 2 months of age. **c-d**,whole ovarian sections with different stages of follicle development. **e-f**, the most advanced stage of follicle development in control (corpus luteum) and DKO ovaries (Preantral follicle). **g-h**, antral follicles from control and DKO ovaries (hemorrhagic). Asterisks indicate the presence of corpora lutea.n=7 for all control specimens and n=3 for the *Dhh/Ihh* DKO specimens. Scale bar: a-b, 1 mm; c-h, 200 mm.

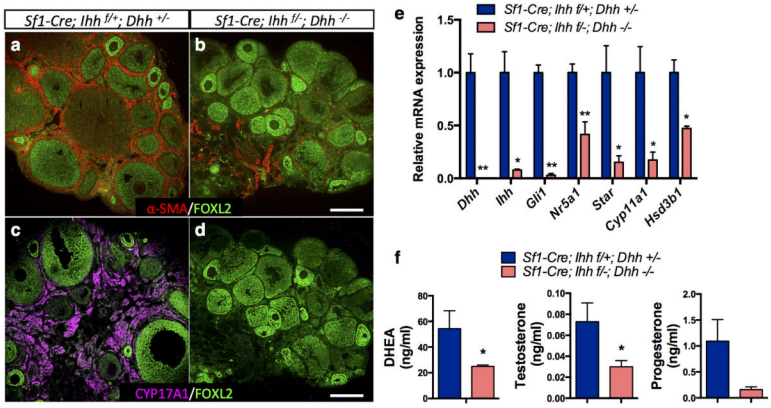

Figure 6. *Dhh* and *Ihh* are required for theca cell development in the ovary

a-d, Immunofluorescence of α-SMA in red (a, b), CYP17A1 in magenta (c, d) and FOXL2 in green in *Dhh/Ihh* DKO (n=3) and control ovaries (n=7). α-SMA is a marker for smooth muscle cell. CYP17A1 is a marker for androgen-producing theca cells and FOXL2 marks granulosa cells. Scale bar: 200 mm. **e**, qPCR analysis of gene expression for Hedgehog signaling components (*Dhh, Ihh*, and *Gli1*), and genes associated with steroidogenesis (*Nr5a1*, *Star*, *Cyp11a1*, and *Hsd3b1*) in control (n=4) and DKO ovaries (n=3). Two-tailed Student's *t*-test was used. *P < 0.05; **P < 0.01. **f**, Serum levels of DHEA, testosterone and progesterone in control (n=7) and *Dhh/Ihh* DKO female mice (n=3). *P < 0.05. Two-tailed Student's *t*-test was used and values in all graphs are presented as means±s.e.m.

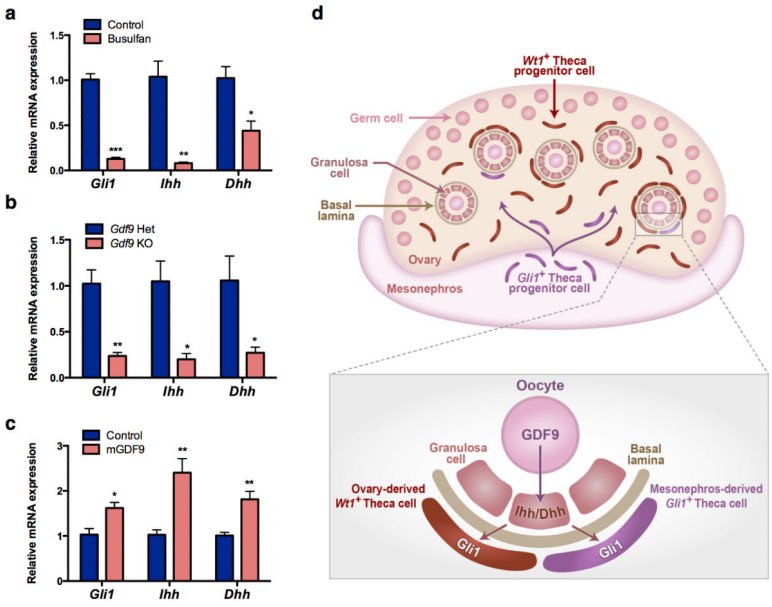

Figure 7. *Gli1* expression in the theca progenitor cells is induced by oocyte-derived factor GDF9 through Hedgehog signaling in granulosa cells

a, qPCR analysis of *Gli1*, *Ihh* and *Dhh* mRNA expression in the control (n=4) and busulfan-treated ovaries (n=3). Two ovaries were pooled as n of 1 and three times independent experiments were repeated. **b**, qPCR analysis of *Gli1*, *Ihh* and *Dhh* mRNA expression in control (n=3) and *Gdf9* knockout ovaries (n=3). **c**, qPCR analysis of *Gli1*, *Ihh* and *Dhh* mRNA expression in the E18.5 oocyte-depleted ovaries (busulfan-treated) cultured with (n=5) or without (n=5) recombinant mouse GDF9 protein (60 ng/ml). The expression level in oocyte-depleted ovaries without GDF9 (Control) was set as 1. Two ovaries were pooled as n of 1 and two times independent experiments were repeated. *P < 0.05; **P < 0.01; ***P < 0.001; Two-tailed Student's *t*-test. Values in all graphs are presented as means ±s.e.m. **d**, Proposed model for the origins and establishment of theca cell lineage in the mouse ovary.